



Targeting the superoxide/nitric oxide ratio by L-arginine and SOD mimic in rat diabetic skin

Aleksandra Jankovic, Carla Ferreri, Milos Filipovic, Ivana Ivanovic-Burmazovic, Ana Stancic, Vesna Otasevic, Aleksandra Korac, Biljana Buzadzic & Bato Korac

To cite this article: Aleksandra Jankovic, Carla Ferreri, Milos Filipovic, Ivana Ivanovic-Burmazovic, Ana Stancic, Vesna Otasevic, Aleksandra Korac, Biljana Buzadzic & Bato Korac (2016): Targeting the superoxide/nitric oxide ratio by L-arginine and SOD mimic in rat diabetic skin, Free Radical Research, DOI: [10.1080/10715762.2016.1232483](https://doi.org/10.1080/10715762.2016.1232483)

To link to this article: <http://dx.doi.org/10.1080/10715762.2016.1232483>



Accepted author version posted online: 05 Sep 2016.
Published online: 05 Sep 2016.



[Submit your article to this journal](#)



[View related articles](#)



[View Crossmark data](#)

**Targeting the superoxide/nitric oxide ratio by L-arginine and SOD mimic
in rat diabetic skin**

Aleksandra Jankovic^a, Carla Ferreri^b, Milos Filipovic^c, Ivana Ivanovic-Burmazovic^d, Ana Stancic^a,
Vesna Otasevic^a, Aleksandra Korac^e, Biljana Buzadzic^a and Bato Korac^{a,e}

^aUniversity of Belgrade, Department of Physiology, Institute for Biological Research “Sinisa Stankovic”, Belgrade, Serbia;

^bISOF, BioFreeRadicals Group, Consiglio Nazionale delle Ricerche, Bologna, Italy;

^cUniversity of Bordeaux IBGC, UMR 509, France;

^dFriedrich-Alexander-University of Erlangen-Nürnberg, Department of Chemistry and Pharmacy, Erlangen, Germany;

^eUniversity of Belgrade, Faculty of Biology, Centre for Electron Microscopy, Belgrade, Serbia.

Address for correspondence: Professor Bato Korac
University of Belgrade
Institute for Biological Research “Sinisa Stankovic”
Department of Physiology
Bulevar despota Stefana 142
11060 Belgrade
Serbia
TEL.: (381-11)-2078-307
FAX: (381-11)-2761-433
E-mail: koracb@ibiss.bg.ac.rs

Abstract

Setting the correct ratio of superoxide anion ($O_2^{\cdot-}$) and nitric oxide ($\cdot NO$) radicals seems to be crucial in restoring disrupted redox signaling in diabetic skin and improvement of $\cdot NO$ physiological action for prevention and treatment of skin injuries in diabetes. In this study we examined the effects of L-arginine and manganese(II)-pentaazamacrocyclic superoxide dismutase (SOD) mimic – M40403 in diabetic rat skin. Following induction of diabetes by alloxan (blood glucose level ≥ 12 mmol l^{-1}) non-diabetic and diabetic male Mill Hill hybrid hooded rats were divided into three subgroups: (i) control, and receiving: (ii) L-arginine, (iii) M40403. Treatment of diabetic animals started after diabetes induction and lasted for 7 days. Compared to control, lower cutaneous immunoexpression of endothelial NO synthase (eNOS), heme oxygenase 1 (HO1), manganese SOD (MnSOD) and glutathione peroxidase (GSH-Px), in parallel with increased NFE2-related factor 2 (Nrf2) and nitrotyrosine levels characterized diabetic skin. L-arginine and M40403 treatments normalized alloxan-induced increase in nitrotyrosine. This was accompanied by the improvement/restitution of eNOS and HO1 or MnSOD and GSH-Px protein expression levels in diabetic skin following L-arginine, i.e. SOD mimic treatments, respectively. The results indicate that L-arginine and M40403 stabilize redox balance in diabetic skin and suggest the underlying molecular mechanisms. Restitution of skin redox balance by L-arginine and M40403 may represent an effective strategy to ameliorate therapy of diabetic skin.

Key words: diabetes, nitric oxide, superoxide, SOD mimic, skin redox balance

Introduction

Diabetes mellitus is a chronic metabolic disease of complex etiology caused by deficiency in insulin or insulin action, characterized by elevated levels of blood glucose. In the skin, sustained hyperglycemia leads to a series of pathological/biochemical processes resulting in inflammation, redox disbalance, changes in the composition of extracellular matrix, and functional deficit of proteins, ultimately developing in clinical symptoms: micro- and macro-angiopathy, polyneuropathy and changes in the connective tissue texture [1]. More than 70% diabetes patients suffer from pathologic skin changes. Chronic inflammation, ulcers and wounds in the skin during the course of disease may progress in gangrene and/or necrosis. Thus, it is of great importance to find more effective therapies to avert the development and/or progression of diabetic complications in the skin.

Insults from increased levels of reactive oxygen and/or nitrogen species (ROS/RNS) play a key role in development of diabetic complications [2–4], yet, the classic antioxidants failed to show significant benefits. An innovative approach for controlling ROS excess appeared in the recent years relies on the redox-active mechanism-based agents. Different superoxide dismutase (SOD) mimics have been used in diverse pathophysiological conditions associated with high superoxide anion ($O_2^{\cdot-}$) level [5–7], including diabetes [8–11]. Initially designed to relief from excess $O_2^{\cdot-}$, growing data suggest that decreased formation of two-electron oxidants, such as peroxynitrite ($ONOO^-$), the subsequent nitr(ox)ative stress, and the restored signaling by nitric oxide ($\cdot NO$) underline the therapeutic benefits of these agents [8,10,12–15].

The essential biological processes in the skin, such as microcirculation and innervation, proliferation of fibroblasts and keratinocytes, synthesis of collagen and immune response are regulated by $\cdot NO$ [16–21]. There are strong indications that impaired function of $\cdot NO$ in these processes leads to poor skin nutrition and altered thermoregulation, dysfunction of somatosensory and nociceptive system, reduced regenerative capacity and susceptibility to infections [21,22]. The availability of $\cdot NO$ to act in redox signaling is determined by its (i) site and level of synthesis, *in vivo* dominantly by L-arginine oxidation in a reaction catalyzed by nitric oxide synthases (NOSs) [23,24], and (ii) interactions with different biotargets, like ferrous anion (heme and non-heme), thiyl radicals, O_2 and $O_2^{\cdot-}$ [25,26]. The reaction with $O_2^{\cdot-}$ in different pathophysiological conditions is prime antagonist of physiological $\cdot NO$ actions, since those two radicals combine at a rate $k \sim 10^9\text{--}10^{10} \text{ M}^{-1} \cdot \text{s}^{-1}$, exceeding the rate of interactions of $\cdot NO$ with all known biotargets, and the $O_2^{\cdot-}$ dismutation reaction catalyzed by native SODs. Notably, a study of Luo et al. [22] showed that gene therapy of either

endothelial NOS (eNOS), augmenting the constitutive NOS activity, or manganese SOD (MnSOD), that inhibits cutaneous $O_2^{\bullet-}$ excess, accelerated healing in the skin of type I diabetic mice. This indicated that a non-physiological ratio of $O_2^{\bullet-}$ and $\bullet NO$ may be important in the pathophysiology of diabetic complications in the skin. Thus, deeper understanding of enzymatic and nonenzymatic pathways that determine the levels of $O_2^{\bullet-}$ and $\bullet NO$ in the diabetic skin is essential in their targeting.

The current study was aimed to broaden the knowledge about the molecular mechanisms affecting $O_2^{\bullet-}$ / $\bullet NO$ balance in skin in the early phase of diabetes induction. In particular, the study was designed to test in an animal model the ability to pharmacologically tackle the $O_2^{\bullet-}$ / $\bullet NO$ ratio and to increase $\bullet NO$ bioavailability in diabetic skin by supplementation with L-arginine and manganese(II)-pentaazamacrocyclic SOD mimic - M40403.

Methods

Animals and diabetes induction

Male Mill Hill hybrid hooded, 3-month-old rats (*Rattus norvegicus*, Berkenhout, 1769) were used. The animals were kept on a 12/12 reverse light/dark cycle, with standard chow diet and water ad libitum. They were divided into two groups: diabetic and non-diabetic rats. Alloxan (Sigma, Germany) was applied to induce diabetes. After a 12 h fasting period, animals received a single alloxan dose of 120 mg (kg body weight⁻¹) i.p. The rats with blood glucose level ≥ 12 mmol l⁻¹, measured by glucose oxidase reagent strips (GlucoSure test, 'Prizma', Kragujevac, Serbia) were considered diabetic. Also, diabetes was confirmed by lower serum insulin level and body weight (diabetic rats had as to non-diabetic lower insulin (14±2 mU/L vs. 56±14 mU/L and negative body weight gain (-27±3 g vs. 19±3 g), as observed previously in a similar experimental settings [27]. Both diabetic and non-diabetic group were additionally separated into three subgroups. One subgroup was receiving 2.25% L-arginine (Sigma, Germany) in drinking water for 7 days. The second subgroup was receiving M40403 in a dose of 5 mg/kg/day i.p. The synthesis and purification of M40403 were carried out at the Institute of Inorganic Chemistry at the Friedrich-Alexander-University of Erlangen-Nürnberg, following a procedure of Salvemini et al. [5]. M40403 was dissolved in 23 mM sodium bicarbonate buffer pH 8.34. The third subgroup was receiving 23 mM sodium bicarbonate buffer pH 8.34 i.p. and served as a control. The rats were treated for one week. Treatment of diabetic rats started after diabetes induction. Each experimental group consisted of six animals. The experiments were approved by the Ethical Committee for the

Treatment of Experimental Animals of the Institute for Biological Research 'Siniša Stanković', Belgrade.

Samples collection and preparation

After 7 days of treatment, body weight and blood glucose level were determined and the rats killed by decapitation. Blood was collected, allowed to clot and centrifuged (3500 g) to prepare serum. Serum insulin levels were estimated by radioimmunoassay (INEP, Belgrade, Serbia). The skin was dissected out within 3 min of death and thoroughly rinsed with physiological saline to remove traces of blood. Only white parts from the dorsal side were taken after cutting the hair with an electric clipper. Hypodermis was removed with a scalpel, and remained skin portions were prepared for Western blot analysis, light and confocal microscopy. Immediately after dissection and washing, a part of skin tissue was fixed in 10 % formaldehyde at 4 °C overnight and processed routinely for embedding in paraplast (5h, on 58 °C). For Western blot analysis, a portion of the tissue weighting 1.5 g was homogenized (Ultra/Turrax homogeniser, Janke und Kunkel Ka/Werke, Staufen, Germany, 0-4 °C) in 5 ml 0.25 M sucrose, 0.1 mM EDTA and 50 mM Tris-HCl buffer, pH 7.4, which contained 10 µg mL⁻¹ protease inhibitor cocktail (Roche Diagnostic GmbH, Mannheim, Germany). The homogenates were sonicated for 15 s at 40 kHz and were centrifuged at 38000 g for 90 min. The protein concentration in the supernatant was estimated by the method of Lowry et al. [28].

SDS-PAGE and Western blotting

Ten-microgram protein aliquots were boiled, electrophoresed in SDS-polyacrylamide gel, and transferred to Hybond-P polyvinylidene fluoride membranes (Amersham, Piscataway, NJ, USA). The nonspecific binding sites of the membranes were blocked by 5% BSA in TBS (200 mM Tris, 1.5 M NaCl, pH 7.4) for 1 h at room temperature. Then, the blots were incubated with a specific primary antibody in TBS-T (0.2% Triton X-100 and 5% BSA in TBS) against the following: copper zinc SOD (CuZnSOD, sc-11407; 1:300), purchased from Santa Cruz Biotechnology; CA, USA, MnSOD (MAB4081; 1:1000) purchased from Chemicon International, Temecula, CA, USA; catalase (CAT, ab18771; 1:5000), glutathione peroxidase (GSH-Px, ab16798; 1:2000); NFE2-related factor 2 (Nrf2, ab31163; 1:1000) or β actin (ab8226; 1:1000), purchased from ABCAM (Cambridge, UK). The sample was incubated overnight at 4 °C followed by a 2 h incubation period at room temperature with a horseradish peroxidase-conjugated IgG secondary antibody. The goat-anti mouse secondary

antibody (Santa Cruz Biotechnology) was used to detect MnSOD and β actin, while the goat-anti rabbit secondary antibody (Santa Cruz Biotechnology) was used to detect CuZnSOD, CAT, GSH-Px. The protein bands were visualized using a chemiluminescence detection system from Amersham (API, Indianapolis, IN, USA). The intensity of the bands was quantified using ImageQuant software. The volume was the sum of all the pixel intensities within a band, i.e., 1 pixel = 0.007744 mm². We averaged the ratio of dots per band for the target protein and for β actin in the corresponding samples from three similar independent experiments and we expressed the ratios relative to that of the control group, which was standardized to be 100%. The data were then statistically analyzed.

Immunohistochemical staining

Paraffin-embedded 7 μ m-thick sections of skin tissues were deparaffinized by xylene and rehydrated in graded ethanol. After antigen retrieval in 10 mM citrate buffer (20 minutes in a microwave oven) and washing with phosphate buffered saline (PBS), endogen peroxidase blocking was performed in 3% hydrogen peroxide (H₂O₂) in methanol for 10 min. After thorough rinsing, the sections were incubated overnight at 4 °C with anti-antibodies in PBS, followed by three 5 min PBS washes. Primary antibodies used in this study were: anti-heme oxygenase-1 (HO1, 1:200; Abcam); anti-heme oxygenase-2 (HO2, 1:200; Abcam); anti-eNOS (5 μ g/ml; Abcam), anti-neuronal NOS (nNOS, 1:50; Abcam) and anti-inducible NOS (iNOS, 1:200; Santa Cruz Biotechnology) and anti-nitrotyrosine (1:100; Abcam). Immunodetection was assessed by the Dako LSAB Universal Kit (Dako Scientific, Glostrup, Denmark). After three PBS washes of 5 min each, sections were incubated with 0.012% H₂O₂ and 0.05% diaminobenzidine (Sigma-Aldrich Chemie, Munich, Germany) in PBS for 10 min in dark. The sections were rinsed in distilled water, counterstained with hematoxylin, mounted and examined with a Leica DMLB microscope (Leica Microsystems, Wetzlar, Germany). The specificity of the immune reaction, for both immunofluorescence and routine immunohistochemistry, was tested by replacing the primary antibody with a non-immune rabbit serum or by incubating the sections with the secondary antibody alone. The quantitative evaluation of antibody staining intensity in skin sections was analysed according to Varghese et al. [29] using ImageJ program.

Expression as well as the localization of Nrf2 was detected by confocal microscopy. Paraffin-embedded 7- μ m-thick sections of rat skin samples were deparaffinized and rehydrated. After antigen retrieval in 10mM citrate buffer (5 minutes in the microwave oven) and washing in PBS, sections were incubated with normal goat serum (1:100; ab7481;

Abcam) for 1 hour. This was followed by an overnight incubation at 4 °C with antibodies to Nrf2 (1µg/ml; Abcam) overnight at 4 °C. After rinsing in PBS, sections were labelled with Alexa Fluor® 633-conjugated goat-anti rabbit secondary antibodies (1:400; Molecular Probes, NY, USA) for 1h. SITOX® orange dye (Leiden, The Netherlands) was used to label cell nuclei (red) at a 1/200 dilution for 1h. After washing with PBS for 20 minutes, the slides were mounted with Mowiol (Sigma Aldrich). Confocal images were acquired with a Leica TCS SP5 confocal laser scanning microscope (Leica Microsystems) in sequential mode to avoid cross talk between channels. The double-stained samples were excited with 633- and 547-nm light, respectively. The specificity of immunostaining, for both immunofluorescence and routine immunohistochemistry, was tested by the omission of primary antibodies.

Statistics

One-way analysis of variance (ANOVA) was used for a within group comparison of the data from the molecular analysis. If the F test showed an overall difference, Tukey's t-test was used to evaluate the significance of the differences. Statistical significance was accepted at $P < 0.05$.

Results

Body weight variation

Figure 1 summarizes changes of body weight in non-diabetic and diabetic animals. A significant decrease of body weight was observed in all diabetic groups of rats, as compared with non-diabetic control ($P < 0.001$). Also, body weight decrease of diabetic animals was significantly lower in L-arginine-treated rats, as compared to untreated ones ($P < 0.05$).

Expression pattern of eNOS in the rat skin

Figure 2 shows the results of immunohistochemical detection of eNOS. In the control rats eNOS immunopositivity was evident in the epidermis and in the some parts of the dermis, especially in the endothelium of blood vessels (Figure 2a). In contrast to this control pattern, eNOS expression in diabetic untreated rats was markedly reduced ($P < 0.001$) (Figure 2b). L-argininine in non-diabetic rats intensified eNOS immunostaining, particularly in the germinative layer of the epidermis (Figure 2c; $P < 0.05$), whereas the same treatment in diabetic animals (Figure 1d) normalized levels of eNOS in the epidermis. SOD mimetic in non-diabetic animals did not affect eNOS immunopositivity relative to control group (Figure

2e), whereas in comparison to untreated diabetic group SOD mimetic slightly improved eNOS immunostaining in the upper epidermal layers (Figure 2f).

Expression patterns of iNOS and nNOS in the rat skin

Significant protein expression of iNOS was observed in the keratinocytes and some dermal cells in the skin of the control rats (Figure 3, panel A, a). Compared to this, immunopositivity for iNOS was significantly reduced ($P < 0.01$) in the epidermis of diabetic, untreated rats (Figure 3, panel A, b, inset). In non-diabetic animals L-arginine intensified immunostaining for iNOS (Fig 3, panel A, c) as compared to controls, whereas in diabetic animals a slightly intensified iNOS immunopositivity was observed after the L-arginine treatment ($P < 0.05$), as compared to untreated diabetic rats (Figure 3, panel A, d). In comparison with the control, SOD mimetic reduced iNOS immunopositivity in the epidermis (Figure 3, panel A, e, inset). On the other hand, 7-day treatment of diabetic rats with SOD mimetic slightly intensified iNOS expression in the upper layer of the epidermis as compared to untreated diabetic animals (Figure 3, panel A, f, inset). Similarly as for iNOS, only a weak immunohistochemical reaction for nNOS was observed in the epidermis of the control rats (Figure 3, panel B, insets). There was not a significant change in the nNOS immunostaining in diabetes as compared to control rats, as well as after the L-arginine or SOD mimetic treatments (Figure 3, panel B, b-f).

Change of antioxidant enzymes expression

Antioxidant defense enzymes are presented in Figure 4. It can be seen that protein expression levels of MnSOD and GSH-Px were significantly lower in diabetic rat skin than in the non-diabetic control ($P < 0.05$). In non-diabetic rats L-arginine and SOD mimetic had no effect on the protein levels of MnSOD and GSH-Px compared to the corresponding non-diabetic control, whereas in diabetic animals, M40403 normalized protein levels of both MnSOD and GSH-Px. The protein expression levels of CuZnSOD and CAT were not affected in diabetic skin. Treatments with L-arginine and SOD mimetic decreased the level of CuZnSOD ($P < 0.05$), but increased the level of CAT ($P < 0.05$) in diabetic rat skin as compared to non-diabetic control and untreated diabetic rats.

Tyrosine nitration

In vivo peroxynitrite and other RNS production is indicated by the presence of nitrotyrosine-containing proteins in the tissues. Strong immunopositive reaction for

nitrotyrosine could be detected in the sections of skin from diabetic rats but not from control (nondiabetic) ones (Figure 5 a, b). Tyrosine nitration immunolabelling was the most intense in the epidermal layers and specific cells in the dermis, in particular endothelial cells of the dermal capillaries (Figure 5b). L-arginine treatment of non-diabetic animals significantly increased nitrotyrosine immunoeexpression in the cytoplasm of cells of the epidermal layers, as compared to the control animals (Figure 5c; $P < 0.001$). Increased immunostaining is also observed in some cells of the dermis, macrophages and capillary endothelium. However, L-arginine in diabetic animals significantly reduced nitrotyrosine immunostaining compared to diabetic, untreated rats (Figure 5d; $P < 0.05$). SOD mimetic treatment of non-diabetic animals showed effects similar to those induced by L-arginine (Figure 5e; $P < 0.01$). However, in diabetic animals the SOD mimetic markedly reduced immunostaining for nitrotyrosine in comparison with the untreated diabetic group (Figure 5f; $P < 0.001$).

Immunohistochemical detection of HO1 and HO2

Figure 6 shows the results of immunohistochemical detection of HO1 and HO2. A strong immunopositivity for HO1 is observed in epidermal layers and some dermal cells of the control rats (Figure 6, panel A, a). However, HO1 immunopositivity was significantly reduced in diabetic rats (Figure 6, panel A, b). As compared to untreated diabetic group, both applied treatments, L-arginine ($P < 0.01$) and SOD mimetic slightly increased HO1 immunopositive reaction. In contrast to strong and specific immunoreaction for HO1, there was only a faint reaction for HO2 in the skin sections of investigated groups (Figure 6, panel B).

Localization and protein expression levels of Nrf2

The results of immunofluorescence analysis of Nrf2 in skin sections taken from non-diabetic rats showed a signal for Nrf2 in cells of both the epidermis and some dermal cells (Figure 7, a). The actual activity of Nrf2 protein was complemented by the subsequent staining of cell nuclei, which indicated that Nrf2 protein in the skin of non-diabetic rats is localized mostly in the cytoplasm of the keratinocytes (Figure 7, a).

Compared with this immunostaining pattern in the non-diabetic rat skin, a significantly stronger immunofluorescent reaction was detected in the epidermal cells of diabetic rat skin (Figure 7, a). Analysis of the protein expression levels of Nrf2 by Western blot and further quantification showed a significantly higher expression of Nrf2 in the skin of diabetic, compared to non-diabetic rats ($P < 0.01$) (Figure 7, b).

As compared to both non-diabetic control and untreated diabetic group, L-arginine treatment did not affect significantly protein expression of Nrf2. However, SOD mimetic displayed significant effects on Nrf2 protein expression levels in both non-diabetic and diabetic rats. Namely, SOD mimetic treatment of non-diabetic rats increased the amount and the nuclear localization of Nrf2 in the epidermal cells. On the other hand, 7-day SOD mimetic treatment of diabetic rats attenuated Nrf2 increase induced in diabetic conditions.

Discussion

Despite vast evidences that excess levels of ROS/RNS, largely due to hyperglycemia and hyperlipidemia, cause tissues redox imbalance, which exacerbates the development of diabetes and its complications in different tissues, clinical trials with classic antioxidants (like vitamin E) failed to demonstrate benefit. The present study contributes to the understanding of the molecular mechanisms affecting $O_2^{\cdot-}/NO$ balance in skin in the early phase of diabetes induction. The study showed that diminished expression of eNOS, MnSOD, GSH-Px and HO1, in parallel with increased Nrf2 expression and nitrotyrosine levels, characterize diabetic, as compared to non-diabetic, rat skin. Significantly, results also indicated that targeting of $O_2^{\cdot-}/NO$ ratio by SOD mimic and/or L-arginine in diabetic skin may be an effective pharmacological strategy in preventing/curbing redox imbalance in diabetic skin. Precisely, results revealed that SOD mimic and L-arginine supplementation normalized nitrotyrosine levels in diabetes which points on the restoration of the $O_2^{\cdot-}/NO$ ratio to the physiological. Observed redox reset could be attributed to direct effects of L-arginine and SOD mimic on the levels of $O_2^{\cdot-}/NO$, as well as to indirect effects of these redox active compounds on the upregulation of eNOS and HO1, i.e. MnSOD and GSH-Px expression, respectively, by complex transcription mechanisms. Details of disturbed skin redox homeostasis after the diabetes onset and the specific effects of L-arginine and SOD mimic treatments are discussed further.

Some therapeutic effect achieved by herbal/fungal (*Strobilanthes crispus* extracts or *Ganoderma lucidum* polysaccharide) and other natural products, like xanthohumol, in the treatment of diabetic skin complications at least in part involves suppression of cutaneous antioxidant enzymes inactivation and protein nitration [30–32]. Besides, a systemic administration of L-arginine induced regeneration of β cells in rats treated with alloxan [27] and improved healing capacity of skin in aged individuals [33], while a study of Luo et al. [22] showed that gene therapy of eNOS or MnSOD accelerated healing in the skin of type I

diabetic mice. All these data indicated that a non-physiological $O_2^{\cdot-}/NO$ ratio might be important in dysfunction of diabetic skin.

The bioavailability of NO is determined by its site and level of synthesis, *in vivo* dominantly by oxidation of L-arginine, a reaction catalyzed by NOSs [23,24]. Although diminished physiological levels of NO underlie some of the pathophysiological changes in diabetes, the expression pattern of NOSs is mostly examined at the site of wound tissue, and not in the unwounded diabetic skin tissue, which is important in revealing the earliest signs of skin dysfunction in diabetes. The present findings showed that diabetes shuts down expression of eNOS in all skin compartments dermis and epidermis, and to a lesser extent decreases the immunoeexpression of iNOS in epidermis. A profound decrease of eNOS expression in the dermal vessels may deteriorate vasodilatory action of NO and the perfusion of diabetic skin, as it is previously observed [34], while attenuation of eNOS and iNOS observed in the epidermis may underlie the impaired function of NO in the re-epithelialization capacity of the diabetic skin [20,21,35].

Next, we examined the expression levels of the main antioxidant enzymes involved in $O_2^{\cdot-}/H_2O_2$ scavenging and found decreased levels of MnSOD and GSH-Px protein expression in the skin of diabetic rats. Consistently, different animal [30,31] and human [36] models indicated dysfunction/inactivation of MnSOD and GSH-Px in the diabetic skin. Rising hyperglycemia is known to increase oxidative pressure in tissues through overproduction of $O_2^{\cdot-}$ [4,22,37] and by impaired $O_2^{\cdot-}/H_2O_2$ scavenging capacity [36,38,39]. Thus, low expression of mitochondrial enzymes MnSOD and GSH-Px observed in the skin of diabetic rats may add to hyperglycemia-associated production of $O_2^{\cdot-}$ and its dismutation product, H_2O_2 , especially at the sites of mitochondria. Accordingly, these organelles [4,37], in addition to NADPH oxidases [22] represent the major sites of $O_2^{\cdot-}$ burden in diabetic skin.

Superoxide levels, increasing in parallel with hyperglycemia may be regarded as the main antagonist of NO -signaling in diabetic skin [22]. Namely, when occurring simultaneously and in equimolar levels, these two radical species combine, as $O_2^{\cdot-}$ has a greater reactivity with NO than with SOD [40] that otherwise keeps control levels of $O_2^{\cdot-}$ [41]. As a consequence, low levels of MnSOD seen in diabetic skin may increase the likelihood of $NO/O_2^{\cdot-}$ interaction. The product of NO and $O_2^{\cdot-}$ combination is the highly reactive oxidant peroxynitrite - $ONOO^-$, that at physiological pH, decays to form hydroxyl radicals (OH) and nitrogen dioxide radical (NO_2) [42] the latter of which nitrates tyrosine residues in different proteins potentially leading to their inactivation. Indeed, the results revealed intensive nitrotyrosine staining in diabetic rat skin. Increased nitrotyrosine

immunoreactivity per se does not prove the $\cdot\text{NO}/\text{O}_2^{\cdot-}$ interaction and ONOO^- increase, since nitrogen dioxide, its derivatives and other reactive nitrogen species resulting from the interaction of $\cdot\text{NO}$ with molecular oxygen or thyl radicals may give rise to nitrotyrosine levels [43]. In addition, a major end product of $\cdot\text{NO}$ metabolism - nitrite (NO_2^-) can increase tyrosine nitration in ONOO^- - independent ways [44]. Thus, strong immunoreactivity of nitrotyrosine in non-diabetic groups, especially after L-arginine treatment, may be explained by increased level of different RNS. In hyperglycemic conditions, however, increased $\text{O}_2^{\cdot-}$ may be the prevailing in the reaction with $\cdot\text{NO}$, since as above stated, those two radicals combine at near diffusion limited rate, exceeding the rate of interactions of $\cdot\text{NO}$ with all known biotargets. Accordingly, increased levels of nitrotyrosine are frequent in the skin of streptozotocin-induced type 1 diabetic mice [31] and rats [32], and the most likely reflect $\cdot\text{NO}/\text{O}_2^{\cdot-}$ interaction [45]. It has been observed that increasing the level of $\cdot\text{NO}$ toward the $\text{O}_2^{\cdot-}$ level may break their interaction and lower their product - ONOO^- levels [46,47]. Since strategies that increase the ratio of $\cdot\text{NO}$ toward $\text{O}_2^{\cdot-}$ by i) reinforcing $\cdot\text{NO}$ synthetic pathway by L-arginine or ii) resetting the $\text{O}_2^{\cdot-}$ excess by SOD mimic, both normalized nitrotyrosine level in diabetic skin, the current study strongly suggests that nitrotyrosine levels in diabetic rat skin the most likely results from increased levels of $\text{O}_2^{\cdot-}$ and the $\cdot\text{NO}/\text{O}_2^{\cdot-}$ interaction. In addition, the current study highlighted complex molecular mechanisms underlying redox actions of L-arginine and SOD mimic in skin of diabetic rats; these involve restitutions of enzymes involved in $\cdot\text{NO}$ and carbon monoxide (CO) synthesis, and/or antioxidant defense.

An important product of HO1 activity, namely CO, overlaps in biological actions with $\cdot\text{NO}$. By guanylate cyclase activation and cGMP-mediated signaling, CO and $\cdot\text{NO}$ overlaps and may compensate each other deficiency in the modulation of vessel contractility [48] and/or cell proliferation [49], impairment of which may worsen regenerative capacity of diabetic skin. Besides, products of HO and NOS activities - CO and $\cdot\text{NO}$, respectively - reciprocally regulate each other enzymes activity [50,51]. The results of the current study have shown similar tissue localization and decreases of HO1 and eNOS in diabetic- as compared to control rat skin. Importantly, L-arginine, and to a lesser extent, SOD mimic treatments acted by improving/restoring decreased levels of eNOS and HO1 in diabetic skin. All these data clearly showed the importance of the mutual interrelation of eNOS/iNOS and HO1 in the maintenance of $\cdot\text{NO}$ and CO balance in diabetic skin. They motivate additional studies needed for the clarification of the transcriptional mechanisms of NOSs and HO1 upregulation by applied treatments.

Transcription factor Nrf2 plays an important role against the hyperglycemia-induced oxidative damage. Both, *in vitro* [52–54] and *in vivo* [55,56] experimental data showed that this factor is activated in response to rising glycaemia and that impaired Nrf2 signaling in the course of diabetes development contributes to diabetic complications in the skin [57]. Under normal conditions, Nrf2 is constitutively targeted by its negative regulator, Kelch-like ECH-associated protein-1 (Keap-1), for ubiquitination and degradation in the cytosol [58,59]. On the other hand, excess of oxidants and/or electrophiles stabilizes Nrf2 by releasing Keap1 binding, allowing Nrf2 to translocate to the nucleus where it binds to antioxidant response elements and drives expression of antioxidant genes and HO1 [60]. Consistently, data indicate that Nrf2 initially increases early after the diabetes onset [61]. Accordingly with literature, here observed changes in Nrf2 in diabetic skin, together with increase of nitrotyrosine and lowered antioxidant enzymes - MnSOD and GSH-Px, indicate that Nrf2 increase is an early adaptive response to overcome increased oxidants and/or electrophiles levels in diabetic skin. Interestingly, Nrf2 increase in diabetic skin was prevented by SOD mimic treatment. Such effects of SOD mimic on Nrf2 in diabetic skin, might be related by oxidative/nitr(ox)ative pressure relief induced by direct SOD catalytic activity, and by the reinforcement of endogenous MnSOD and GSH-Px expression levels, as observed in diabetic SOD mimic-treated rats, as compared to untreated rats. In turn, it could be speculated that effects of SOD mimic on the upregulation protein expression of MnSOD and GSH-Px in the skin of diabetic rats, could be triggered adaptively to accommodate elevated H₂O₂ production raised by catalytic activity of SOD mimic and by need to maintain some optimal level of mitochondrial MnSOD.

In summary, the results of the current study suggests that L-arginine and SOD mimic treatments reset the nonphysiological $\cdot\text{NO}/\text{O}_2^{\cdot-}$ ratio and suggest key molecular players of their action in diabetic skin. Nevertheless, SOD mimics are redox active compounds with complex chemistry and biology. Also, the effects of L-arginine are mainly attributed to its role in the synthesis of $\cdot\text{NO}$ and $\cdot\text{NO}$ -mediated signaling. Furthermore, L-arginine may influence mammalian target of rapamycin – mTOR signalling [62,63], as well as adenylyl cyclase /cAMP- [64], nuclear factor(NF)-kappaB- [65], mitogen-activated protein kinase-MAPK- [66] mediated signaling pathways thereby modulating protein synthesis and other important cellular processes. Also, L-arginine is a precursor of agmatine, creatine, ornithine and polyamines [67] wich have important roles in collagen synthesis, cellular proliferation and overall skin homeostasis [68]. To further elucidate the mechanisms of specific SOD mimics, as well as of L-arginine on upregulation of enzymes involved in $\cdot\text{NO}$ and CO synthesis and

antioxidant enzymes expression levels in diabetes, additional studies are required, including those pointed to the identification of specific redox-sensitive transcription factors, and research along these lines are in progress.

Acknowledgements

This work was supported by the Ministry of Education, Science and Technological Development of the Republic of Serbia (Grant No 173055) and the European Cooperation in Science and Research (COST Action CM1201).

Disclosure of interest

The authors report no conflicts of interest.

JUST ACCEPTED

References

- [1] Wohlrab J, Wohlrab D, Meiss F. Skin diseases in diabetes mellitus. *J Dtsch Dermatol Ges.* 2007;5:37–53.
- [2] Pacher P, Obrosova IG, Mabley JG et al. Role of nitrosative stress and peroxynitrite in the pathogenesis of diabetic complications. Emerging new therapeutical strategies. *Curr Med Chem.* 2005;12:267–275.
- [3] Pacher P, Szabó C. Role of peroxynitrite in the pathogenesis of cardiovascular complications of diabetes. *Curr Opin Pharmacol.* 2006;6:136–141.
- [4] Giacco F, Brownlee M. Oxidative stress and diabetic complications. *Circ Res.* 2010;107:1058–1070.
- [5] Salvemini D, Wang ZQ, Zweier JL, et al. A nonpeptidyl mimic of superoxide dismutase with therapeutic activity in rats. *Science* 1999;286:304–306.
- [6] Wang ZQ, Porreca F, Cuzzocrea S, et al. A newly identified role for superoxide in inflammatory pain. *J Pharmacol Exp Ther.* 2004;309:869–878.
- [7] Hoehn KL, Salmon AB, Hohnen-Behrens C, et al. Insulin resistance is a cellular antioxidant defense mechanism. *Proc Natl Acad Sci USA.* 2009;106:17787–17792.
- [8] Coppey LJ, Gellett JS, Davidson EP, et al. Effect of M40403 treatment of diabetic rats on endoneurial blood flow, motor nerve conduction velocity and vascular function of epineurial arterioles of the sciatic nerve. *Br J Pharmacol.* 2001;134:21–29.
- [9] Ali DK, Oriowo M, Tovmasyan A, et al. Late administration of Mn porphyrin-based SOD mimic enhances diabetic complications. *Redox Biol.* 2013;1:457–466.
- [10] Stančić A, Otašević V, Janković A, et al. Molecular basis of hippocampal energy metabolism in diabetic rats: the effects of SOD mimic. *Brain Res Bull.* 2013;99:27–33.

[11] Batinic-Haberle I, Tovmasyan A, Roberts ER, et al. SOD therapeutics: latest insights into their structure-activity relationships and impact on the cellular redox-based signaling pathways. *Antioxid Redox Signal*. 2014;20:2372–415.

[12] Batinic-Haberle I, Cuzzocrea S, Reboucas JS, et al. Pure MnTBAP selectively scavenges peroxynitrite over superoxide: comparison of pure and commercial MnTBAP samples to MnTE-2-PyP in two models of oxidative stress injury, an SOD-specific *Escherichia coli* model and carrageenan-induced pleurisy. *Free Radic Biol Med*. 2009;46:192–201.

[13] Janes K, Neumann WL, Salvemini D. Anti-superoxide and anti-peroxynitrite strategies in pain suppression. *Biochim Biophys Acta* 2012;1822:815–821.

[14] Otasevic V, Korac A, Vucetic M, et al. Is manganese (II) pentaazamacrocyclic superoxide dismutase mimic beneficial for human sperm mitochondria function and motility? *Antioxid Redox Signal*. 2013;18:170–178.

[15] Jankovic A, Korac A, Buzadzic B, et al. Targeting the nitric oxide/superoxide ratio in adipose tissue: relevance in obesity and diabetes management. *Br J Pharmacol*. 2016; in press, doi: 10.1111/bph.13498.

[16] Ignarro LJ, Byrns RE, Buga GM, et al. Pharmacological evidence that endothelium-derived relaxing factor is nitric oxide: use of pyrogallol and superoxide dismutase to study endothelium-dependent and nitric oxide-elicited vascular smooth muscle relaxation. *J Pharmacol Exp Ther*. 1988;244:181–189.

[17] Rees DD, Palmer RM, Hodson HF, et al. A specific inhibitor of nitric oxide formation from L-arginine attenuates endothelium-dependent relaxation. *Br J Pharmacol*. 1989;96:418–424.

[18] Knowles RG, Palacios M, Palmer RM, et al. Formation of nitric oxide from L-arginine in the central nervous system: a transduction mechanism for stimulation of the soluble guanylate cyclase. *Proc Natl Acad Sci USA*. 1989;86:5159–5162.

- [19] Bruch-Gerharz D, Ruzicka T, Kolb-Bachofen V. Nitric oxide and its implications in skin homeostasis and disease - a review. *Arch Dermatol Res.* 1998;290:643–651.
- [20] Frank S, Kämpfer H, Wetzler C, et al. Nitric oxide drives skin repair: novel functions of an established mediator. *Kidney Int.* 2002;61:882–888.
- [21] Weller R. Nitric oxide: a key mediator in cutaneous physiology. *Clin Exp Dermatol.* 2003;28:511–514.
- [22] Luo JD, Wang YY, Fu WL, et al. Gene therapy of endothelial nitric oxide synthase and manganese superoxide dismutase restores delayed wound healing in type 1 diabetic mice. *Circulation.* 2004;110:2484–2493.
- [23] Moncada S, Palmer RM, Higgs EA. The discovery of nitric oxide as the endogenous nitrovasodilator. *Hypertension.* 1988;12:365–372.
- [24] Moncada S, Palmer RM, Higgs EA. Biosynthesis of nitric oxide from L-arginine. A pathway for the regulation of cell function and communication. *Biochem Pharmacol.* 1989;38:1709–1715.
- [25] Beckman JS, Koppenol WH. Nitric oxide, superoxide, and peroxynitrite: the good, the bad, and ugly. *Am J Physiol.* 1996;271:C1424–C1437.
- [26] Wink DA, Mitchell JB. Chemical biology of nitric oxide: Insights into regulatory, cytotoxic, and cytoprotective mechanisms of nitric oxide. *Free Radic Biol Med.* 1998;25:434–456.
- [27] Vasilijevic A, Buzadzic B, Korac A, et al. Beneficial effects of L-arginine nitric oxide-producing pathway in rats treated with alloxan. *J Physiol.* 2007;584:921–933.
- [28] Lowry OH, Rosenbrough NJ, Farr AL, et al. Protein measurement with the Folin phenol reagent. *J Biol Chem.* 1951;193:265–275.

- [29] Varghese F, Bukhari AB, Malhotra R, et al. IHC Profiler: an open source plugin for the quantitative evaluation and automated scoring of immunohistochemistry images of human tissue samples. *PLoS One*. 2014;9:e96801.
- [30] Norfarizan-Hanoon NA, Asmah R, Rokiah MY, et al. Effects of *Strobilanthes crispus* juice on wound healing and antioxidant enzymes in normal and streptozotocin-induced diabetic rats. *J Biol Sci* 2009;9:p.662.
- [31] Tie L, Yang HQ, An Y, et al. *Ganoderma lucidum* polysaccharide accelerates refractory wound healing by inhibition of mitochondrial oxidative stress in type 1 diabetes. *Cell Physiol Biochem*. 2012;29:583–594.
- [32] Costa R, Negrão R, Valente I, et al. Xanthohumol modulates inflammation, oxidative stress, and angiogenesis in type 1 diabetic rat skin wound healing. *J Nat Prod*. 2013;76:2047–2053.
- [33] Kirk SJ, Hurson M, Regan MC, et al. Arginine stimulates wound healing and immune function in elderly human beings. *Surgery*. 1993;114:155–159; discussion 160.
- [34] Kuo YR, Wang CT, Wang FS, et al. Extracorporeal shock-wave therapy enhanced wound healing via increasing topical blood perfusion and tissue regeneration in a rat model of STZ-induced diabetes. *Wound Repair Regen*. 2009;17:522–530.
- [35] Stallmeyer B, Anhold M, Wetzler C, et al. Regulation of eNOS in normal and diabetes-impaired skin repair: implications for tissue regeneration. *Nitric Oxide*. 2002;6:168–177.
- [36] Ceriello A, Morocutti A, Mercuri F, et al. Defective intracellular antioxidant enzyme production in type 1 diabetic patients with nephropathy. *Circ Res*. 2000;107:1058–1070.
- [37] Brownlee M. Biochemistry and molecular cell biology of diabetic complications. *Nature*. 2001;414:813–820.

- [38] Ceriello A, Dello Russo P, Amstad P, et al. High glucose induces antioxidant enzymes in human endothelial cells in culture; Evidence linking hyperglycemia and oxidative stress. *Diabetes*. 1996;45:471–477.
- [39] Hodgkinson AD, Bartlett T, Oates PJ, et al. The response of antioxidant genes to hyperglycemia is abnormal in patients with type 1 diabetes and diabetic nephropathy. *Diabetes*. 2003;52:846–851.
- [40] Huie RE, Padmaja S. The reaction of NO with superoxide. *Free Radic Res Commun*. 1993;18:195–199.
- [41] McCord JM, Fridovich I. Superoxide dismutase. An enzymic function for erythrocyte hemocuprein (hemocuprein). *J Biol Chem*. 1969;244:6049-6055.
- [42] Radi R. Peroxynitrite, a stealthy biological oxidant. *J Biol Chem*. 2013;288:26464–26472.
- [43] Halliwell B. What nitrates tyrosine? Is nitrotyrosine specific as a biomarker of peroxynitrite formation in vivo? *FEBS Lett*. 1997;411:157–160.
- [44] Herce-Pagliai C, Kotecha S, Shuker DE. Analytical methods for 3-nitrotyrosine as a marker of exposure to reactive nitrogen species: a review. *Nitric Oxide*. 1998;2:324–336.
- [45] Yagishita Y, Fukutomi T, Sugawara A, et al. Nrf2 protects pancreatic β -cells from oxidative and nitrosative stress in diabetic model mice. *Diabetes*. 2014;63:605–618.
- [46] Goldstein S, Czapski G, Lind J, et al. Effect of NO on the decomposition of peroxynitrite: reaction of N_2O_3 with ONOO $^-$. *Chem Res Toxicol*. 1999;12:132–136.
- [47] Daiber A, Frein D, Namgaladze D, et al. Oxidation and nitrosation in the nitrogen monoxide/superoxide system. *J Biol Chem*. 2002;277:11882–11888.
- [48] Caudill TK, Resta TC, Kanagy NL, et al. Role of endothelial carbon monoxide in attenuated vasoreactivity following chronic hypoxia. *Am J Physiol*. 1998;275:R1025-R1030.

- [49] Morita T, Mitsialis SA, Koike H, et al. Carbon monoxide controls the proliferation of hypoxic vascular smooth muscle cells. *J Biol Chem*. 1997;272:32804–32809.
- [50] Xie QW, Leung M, Fuortes M, et al. Complementation analysis of mutants of nitric oxide synthase reveals that the active site requires two hemes. *Proc Natl Acad Sci USA*. 1996;93:4891–4896.
- [51] Foresti R, Motterlini R. The heme oxygenase pathway and its interaction with nitric oxide in the control of cellular homeostasis. *Free Radic Res*. 1999;31:459–475.
- [52] He X, Kan H, Cai L, et al. Nrf2 is critical in defense against high glucose-induced oxidative damage in cardiomyocytes. *J Mol Cell Cardiol*. 2009;46:47–58.
- [53] Tiang T, Huang Z, Lin Y, et al. The protective role of Nrf2 in streptozotocin-induced diabetic nephropathy. *Diabetes*. 2010;59:850–860.
- [54] Ungvari Z, Bailey-Downs L, Gautam T, et al. Adaptive induction of NF-E2-related factor-2-driven antioxidant genes in endothelial cells in response to hyperglycemia. *Am J Physiol Heart Circ Physiol*. 2011;300:H1133–H1140.
- [55] Zheng H, Whitman SA, Wu W, et al. Therapeutic potential of Nrf2 activators in streptozotocin- induced diabetic nephropathy. *Diabetes*. 2011;60:3055–3066.
- [56] Zhong Q, Mishra M, Kowluru RA. Transcription factor Nrf2- mediated antioxidant defense system in the development of diabetic retinopathy. *Invest Ophthalmol Vis Sci*. 2013;54:3941–3948.
- [57] Bitar MS, Al-Mulla F. A defect in Nrf2 signaling constitutes a mechanism for cellular stress hypersensitivity in a genetic rat model of type 2 diabetes. *Am J Physiol Endocrinol Metab*. 2011;301:E1119–E1129.

[58] Cullinan SB, Gordan JD, Jin J, et al. The Keap1-BTB protein is an adaptor that bridges Nrf2 to a Cul3-based E3 ligase: oxidative stress sensing by a Cul3-Keap1 ligase. *Mol Cell Biol.* 2004;24:8477–8486.

[59] Kobayashi A, Kang MI, Okawa H, et al. Oxidative stress sensor Keap1 functions as an adaptor for Cul3-based E3 ligase to regulate proteasomal degradation of Nrf2. *Mol Cell Biol.* 2004;24:7130–7139.

[60] Itoh K, Chiba T, Takahashi S, et al. An Nrf2/small Maf heterodimer mediates the induction of phase II detoxifying enzyme genes through antioxidant response elements. *Biochem Biophys Res Commun.* 1997;236:313–322.

[61] Tan SM, de Haan JB. Combating oxidative stress in diabetic complications with Nrf2 activators: how much is too much? *Redox Rep.* 2014;19:107–117.

[62] Tan B, Yin Y, Kong X, et al. L-Arginine stimulates proliferation and prevents endotoxin-induced death of intestinal cells. *Amino Acids.* 2010;38:1227–1235.

[63] Yan L, Lamb RF. Signalling by amino acid nutrients. *Biochem Soc Trans* 2011; 39:443–445.

[64] McKnight JR, Satterfield MC, Jobgen WS, et al. Beneficial effects of L-arginine on reducing obesity: potential mechanisms and important implications for human health. *Amino Acids.* 2010;39:349–357.

[65] Kagemann G, Sies H, Schnorr O. Limited availability of L-arginine increases DNA-binding activity of NF-kappaB and contributes to regulation of iNOS expression. *J Mol Med (Berl).* 2007;85:723–732.

[66] Mieulet V, Yan L, Choisy C, et al. TPL-2-mediated activation of MAPK downstream of TLR4 signaling is coupled to arginine availability. *Sci Signal.* 2010;3:ra61.

[67] Morris SM Jr. Arginine: beyond protein. *Am J Clin Nutr.* 2006;83:508S–512S.

[68] Curran JN, Winter DC, Bouchier-Hayes D. Biological fate and clinical implications of arginine metabolism in tissue healing. *Wound Repair Regen.* 2006;14:376–386.

FIGURE CAPTIONS

Figure 1. Changes of body weight in non-diabetic and diabetic rats. The results are the means \pm SEM (n=6 in all groups). Comparison with non-diabetic untreated control: ***p < 0.001; comparison with diabetic untreated control: #p < 0.05. Each bar represents the difference between the initial (day 0) and final (7 days of experiment) body weight.

Figure 2. Immunohistochemical staining for eNOS in the skin of non-diabetic control (a), diabetic untreated (b), non-diabetic L-arginine-treated (c), diabetic L-arginine-treated (d) non-diabetic M40403-treated (e) and diabetic M40403-treated (f) rats. Visualization of the antibody-antigen reaction is accomplished by the use of a secondary antibody conjugated to peroxidase, which catalyses a brown color-producing reaction. Data obtained after quantitative evaluation of immunohistochemistry images represent the mean \pm SEM. *comparison with non-diabetic untreated control, *p < 0.05; ***p < 0.001. #comparison with diabetic untreated control, #p < 0.05. Magnification: 40x orig.; insets 63x. eNOS, endothelial NOS.

Figure 3. Immunohistochemical staining for iNOS and nNOS in the skin of non-diabetic control (a), diabetic untreated (b), non-diabetic L-arginine-treated (c), diabetic L-arginine-treated (d), non-diabetic M40403-treated (e) and diabetic M40403-treated (f) rats. Data obtained after quantitative evaluation of immunohistochemistry images represent the mean \pm SEM. *comparison with non-diabetic untreated control, *p < 0.05; **p < 0.01; ***p < 0.001. #comparison with diabetic untreated control, #p < 0.05. Magnification: 40x orig.; insets 63x. iNOS, inducible NOS; nNOS, neuronal NOS.

Figure 4. Protein content of CuZnSOD, MnSOD, GSH-Px and catalase in skin of non-diabetic and diabetic, untreated, L-arginine treated and M40403 treated rats. The signals from representative Western blot are shown below the graphs. Data obtained after quantification of specific bands, and expressed as % of non-diabetic untreated (control) group taken as 100%, represent the mean \pm SEM. *comparison with non-diabetic untreated control, *p < 0.05. #comparison with diabetic untreated control, #p < 0.05. CuZnSOD, copper zinc superoxide

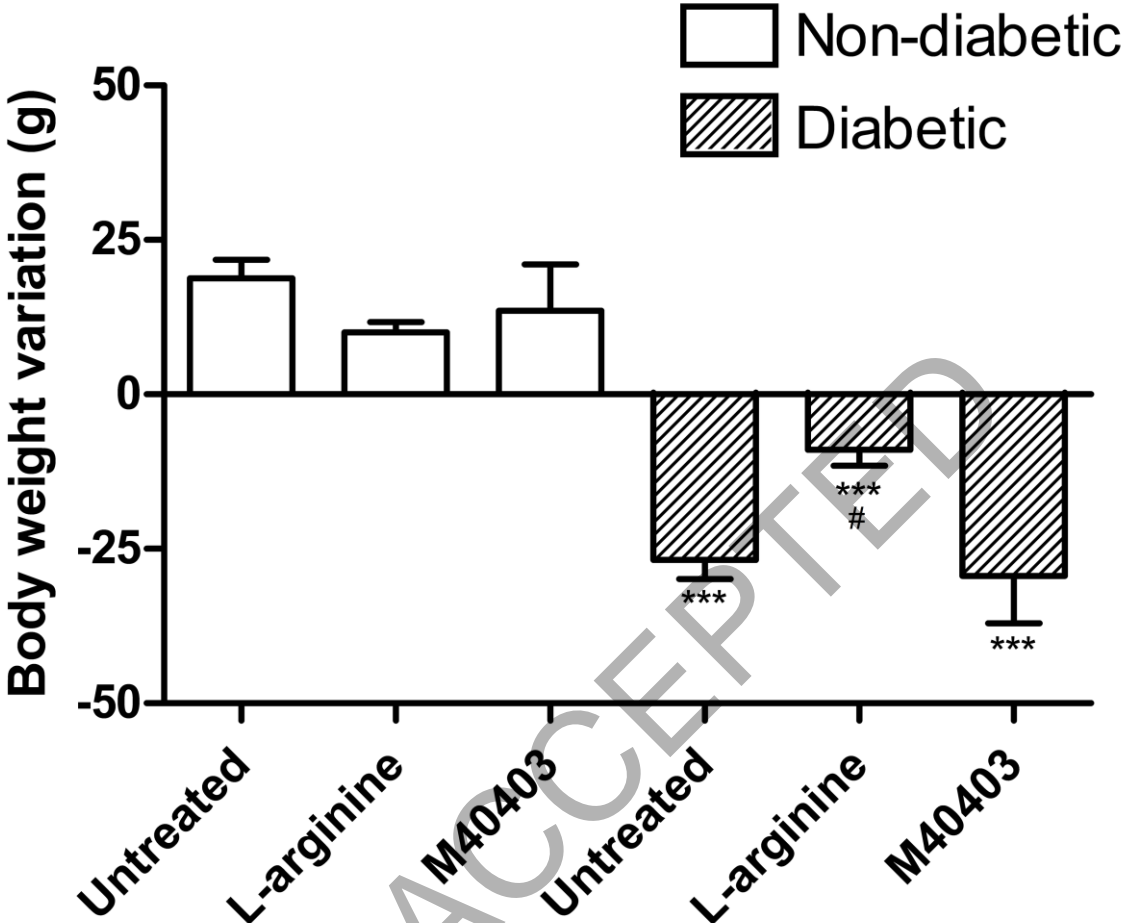
dismutase; MnSOD, manganese superoxide dismutase; GSH-Px, glutathione peroxidase; CAT, catalase.

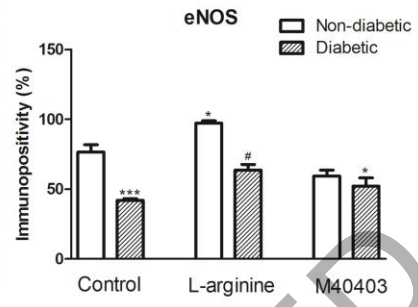
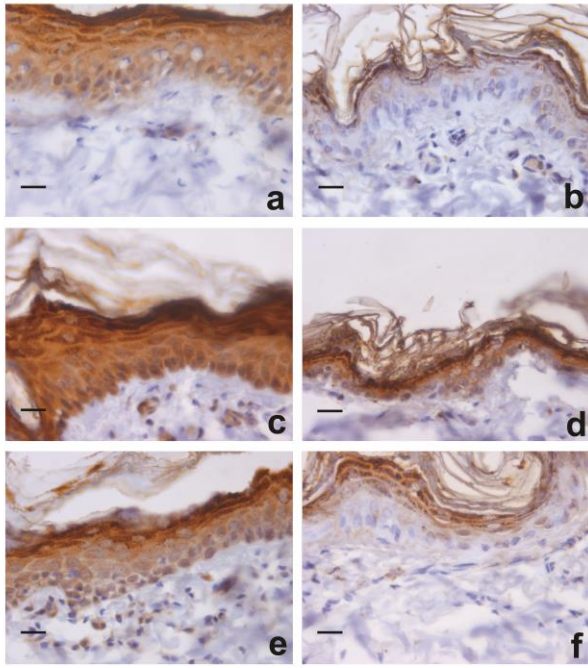
Figure 5. Immunohistochemical staining for 3-nitrotyrosine in the skin of non-diabetic control (a), diabetic untreated (b), non-diabetic L-arginine-treated (c), diabetic L-arginine-treated (d), non-diabetic M40403-treated (e) and diabetic M40403-treated (f) rats. Data obtained after quantitative evaluation of immunohistochemistry images represent the mean \pm SEM. *comparison with non-diabetic untreated control, ** $p < 0.01$; *** $p < 0.001$. #comparison with diabetic untreated control, # $p < 0.05$, ### $p < 0.001$. Magnification: 40x orig.; insets 63x.

Figure 6. Immunohistochemical staining for HO1 (A) and HO2 (B) in the skin of non-diabetic control (a), diabetic untreated (b), non-diabetic L-arginine-treated (c), diabetic L-arginine-treated (d), non-diabetic M40403-treated (e) and diabetic M40403-treated (f) rats. Data obtained after quantitative evaluation of immunohistochemistry images represent the mean \pm SEM. *comparison with non-diabetic untreated control, * $p < 0.05$; ** $p < 0.01$; *** $p < 0.001$. #comparison with diabetic untreated control, # $p < 0.05$; ## $p < 0.01$. Magnification: 40x orig.; insets 63x. HO1, heme oxygenase 1; HO2, heme oxygenase 2.

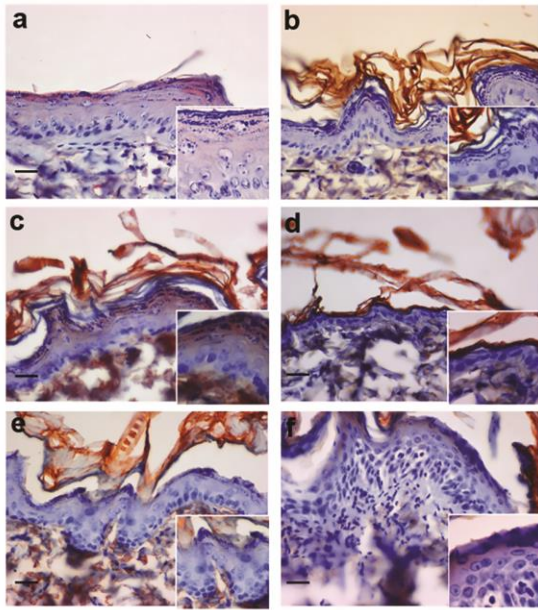
Figure 7. A) Nrf2 protein expression and localization were assessed in the skin from non-diabetic control (a), diabetic untreated (b), non-diabetic L-arginine-treated (c), diabetic L-arginine-treated (d), non-diabetic M40403-treated (e) and diabetic M40403-treated (f) rats. Nrf2 protein expression in the skin of non-diabetic rats (a) is detectable in the epidermis and in fibroblast-like cells in dermis. Nrf2 protein expression was absent in negative staining controls (not shown). In contrast to modest effects of L-arginine, SOD mimetic had significant but inverse effects on Nrf2 protein expression and localization in the skin of non-diabetic and diabetic rats. SOD mimetic increase the level and nuclear localization of Nrf2 in non-diabetic skin, and decrease Nrf2 levels in diabetic skin, as compared to corresponding non-diabetic, i.e. diabetic controls, respectively. B) Protein expression of Nrf2 was analyzed in the skin from untreated non-diabetic, and diabetic controls, and rats treated with L-arginine or with M40403 for 7 days. Representative Western blots and the relative quantification are provided. Protein expression level of Nrf2 increased in the skin of diabetic untreated rats was normalized after M40403 treatment. Data are expressed as mean \pm SEM (n=3) and were obtained from three independent experiments. Significantly different from non-diabetic

control group: **, p < 0.01; ***, p < 0.001; significantly different from diabetic untreated group: #, p<0.05. Nrf2, NFE2-related factor 2.





JUST ACCEPTED

A**B**